J Nanostruct Chem (2017) 7:159–170
DOI 10.1007/s40097-017-0223-8

ORIGINAL RESEARCH

Green synthesis of bimetallic Pt@Cu nanostructures for catalytic oxidative desulfurization of model oil

A. A. Olajire[1] · A. Kareem[1] · A. Olaleke[1]

Received: 29 December 2016 / Accepted: 4 February 2017 / Published online: 21 February 2017

Abstract This study reports the synthesis of bimetallic Pt@Cu nanostructures at elevated temperature of 100 °C using *Alchornea laxiflora* leaf extract (ALLE). The nanostructures have been characterized using UV–vis spectroscopy, high resolution transmission electron microscopy (HRTEM), Fourier Transform Infrared spectroscopy (FTIR), energy dispersive X-ray(EDX) spectroscopy and X-ray diffraction (XRD) techniques. The sizes of the bimetallic Pt@Cu nanostructures range from 1.87 to 2.38 nm with an average particle size of 2.12 ± 0.21 nm, and they crystallized in face-centered cubic (*fcc*) symmetry. The EDX analysis confirms the bimetallism of Pt@Cu nanostructures and individual metals are present in the ratio 2:3. FTIR indicates strong peaks at 3427 cm^{-1} which is attributed to hydroxyl group of polyphenolic compounds in ALLE, and the peak disappeared completely in the FTIR of Pt@Cu nanostructures, thus confirming their significant roles in bioreduction process. Catalytic oxidative property of Pt@Cu nanostructures was investigated by oxidation of a model oil [dibenzothiophene (DBT) dissolved in *n*-heptane] to their corresponding sulfone. Our results show that bimetallic Pt@Cu nanostructures have higher catalytic oxidative activity than the conventional acetic acid that is used in the oxidative desulfurization process. The catalytic oxidative desulfurization activity shown by the Pt@Cu nanostructures promises the potential application in petroleum industry.

✉ A. A. Olajire
olajireaa@yahoo.com

[1] Industrial and Environmental Chemistry Unit, Department of Pure and Applied Chemistry, Ladoke Akintola University of Technology, Ogbomoso, Nigeria

Keywords Green synthesis · Pt@Cu nanostructures · ALLE · Catalytic property · Oxidative desulfurization

Introduction

The search for cheap, safe, low energy and environmental benign route to synthesis of nanoparticles for catalytic conversion of sulfur pollutants in fuel has gotten considerable attention of environmental scientists in recent times. Nanoparticles have been synthesized by various approaches including chemical, physical and biological methods [1–8]. However, the use of physical and chemical methods for nanoparticles synthesis and stabilization though technically effective but not cost-effective and are highly energy intensive [9]. These methods also require the use of toxic and environmentally polluting substances for the syntheses [10, 11]. Thus, green synthesis of nanoparticles using biomaterials is attractive to most scientists due to its simplicity and eco-friendliness. Bimetallic nanostructures are also more attractive for a wide range of catalytic and electrocatalytic applications over their monometallic counterparts due to combined properties of the two individual metals and the synergy that exists between the two metals [12–17].

Platinum-based nanostructures have been given considerable attention due to their potential applications in oil refining, fine chemicals, fuel cell, etc. [16, 18, 19]. In recent times, chemically synthesized Pt@Cu nanostructures have been reported for their enhanced catalytic performance in methanol oxidation and oxygen reduction reactions [20–24]. In view of this background information, there is a need to develop environmental-friendly route to the synthesis of bimetallic Pt@Cu nanostructures with enhanced catalytic properties without the use of toxic

chemicals or intensive energy. Unfortunately, there are no reports on synthesis of bimetallic Pt@Cu nanostructures by plant leaf extract of *Alchornea laxiflora*.

In petroleum industry, hydrodesulfurization (HDS) commonly used for removal of sulfur from fuel could only achieve limited performance due to the presence of refractory sulfur-containing aromatic compounds such as dibenzothiophene (DBT) [25]. Oxidative desulfurization (ODS) is therefore considered as a promising alternative to HDS. In ODS process, DBT is oxidized to corresponding sulfoxide or sulfone using H_2O_2 as oxidant. The oxidant also requires the presence of an efficient catalyst. Organic acids and metal oxides which have been reported in the literature for oxidative desulfurization of model fuel are either not eco-friendly, have low oxidation activity or low utilization efficiency of the oxidants [26–31]. Such problems have led us to develop a green route for the synthesis of Pt@Cu nanostructures using *A. laxiflora* leaf extract (ALLE) as both a reductant and stabilizer, and then compare its catalytic activity with that of the conventional acetic acid used for oxidative desulfurization (ODS) process. No effort has been made so far on the use of biosynthesized Pt@Cu nanostructures as catalyst for oxidative desulfurization of model oil. As part of our growing interest in the application of nanobiotechnology in petroleum industry, we report herein for the first time, the synthesis of bimetallic Pt@Cu nanostructures by *Alchornea laxiflora* leaf extract (ALLE). The catalytic potential of biosynthesized Pt@Cu nanostructures was compared with that of conventional acetic acid catalysts used for oxidative desulfurization of model oil using H_2O_2 as oxidant and acetonitrile as extractant at a temperature of 60 °C (Scheme 1).

Materials and methods

Materials

Chloroplatinic acid hexahydrate ($H_2PtCl_6{\cdot}6H_2O$, Pt content: 38%) and copper (II) sulfate pentahydrate ($CuSO_4{\cdot}5H_2O$; 99% purity) were, respectively, purchased from May and Baker, Dagenham England and Qinhuangdao Lead Chemicals Co. Ltd. (China); and were used as the precursors for the synthesis of bimetallic Pt@Cu nanostructures. Dibenzothiophene ($C_{12}H_8S$) and *n*-heptane were obtained from Sigma-Aldrich. Deionized water was used throughout the study. The plant (*Alchornea laxiflora*) leaves were collected from Ladoke Akintola University of Technology campus. All glass wares were rinsed with concentrated nitric acid (HNO_3) and deionized water followed by drying in the oven. A stock solution of $H_2PtCl_6{\cdot}6H_2O$ was prepared by dissolving 1.0 g in 500 mL deionized water (3.86 mM). Similarly, a stock solution of $CuSO_4{\cdot}5H_2O$ was prepared by dissolving 1.0 g in 500 mL deionized water (8.01 mM).

Extract preparation

The plant (*Alchornea laxiflora*) leaves were rinsed with deionized water and allowed to dry for 2–3 days at laboratory temperature. The dried leaves were cut into pieces and grind into powdery form. The leaf broth solution was prepared by taking 20 g of powdered leaves in a 250 mL Erlenmeyer flask with 200 mL of deionised water and the mixture was boiled at 80 °C for 30 min. The mixture was cooled and vacuum filtered, and the resulting filtrate (extract) was used for further analysis within a week.

Synthesis of Pt@Cu nanostructures

The synthesis of Pt@Cu nanostructures was carried out by mixing 40 mL of the 1 mM aqueous $H_2PtCl_6{\cdot}6H_2O$ solution and 40 mL of the 1 mM aqueous $CuSO_4{\cdot}5H_2O$ solution with magnetic stirring. Subsequently, 20 mL of *Alchornea laxiflora* aqueous leaf extract was added to the platinum and copper ion mixture. The mixture was maintained at 100 °C in a sealed flask to avoid evaporation for 5 h on the hot plate since the temperature catalyses the rate of reduction process. For control experiment, the same amount of platinum and copper solutions was maintained separately under the same reaction conditions. The change in color of the solution as the temperature increases indicates the formation of Pt@Cu nanostructures. The reduced platinum–copper solution was centrifuged at 3000 rpm for 30 min in order to disperse the nanostructures in liquids and purified by repeated centrifugation at 3000 rpm for 15 min. The pellets were washed with distilled water to remove the impurities. The purified Pt@Cu nanostructures were subjected to characterization studies.

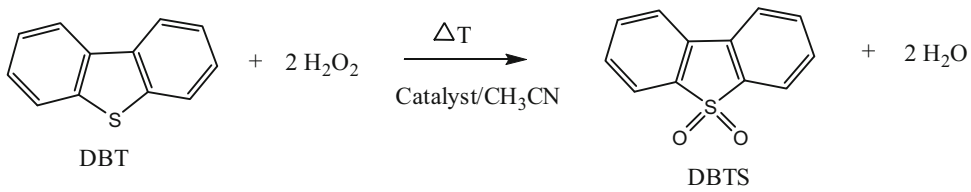

Scheme 1 Oxidation of DBT into DBT sulfone by hydrogen peroxide

Characterization of Pt@Cu nanostructures

The formation of Pt@Cu nanostructures was confirmed by visual color changes and characterized by UV–visible spectrophotometer on a Shimadzu (Cecil 7200 model). The FTIR spectra measurements of dried Pt@Cu nanostructures in the powdered form were measured using IRAffinity 1S Schimadzu spectrometer in KBr pellets. Size and morphology of the as-synthesized Pt@Cu nanostructures were determined by high resolution transmission electron microscope (HRTEM) coupled with Energy dispersive X-ray spectroscopy (EDX) Oxford detector (model X-Max. A JOEL-2100F, USA), at an energy range 0–20 keV. The crystallographic structure of the Pt@Cu nanostructures was probed with powder X-ray diffraction (Bruker D2, Phaser DOC-M88-EXX, 155 V4-07, Germany). XRD analysis was done using Cu–Kα as a source and Ni as a filter media, and K radiation maintained at 1.5406 Å. The XRD data were recorded for 2θ values between 10° and 90°. The crystallite size of the Pt@Cu nanostructures was calculated from the full width at half-maximum (FWHM) of diffraction peaks at $2\theta = 45.2^{o}$, 57^{o} and 68.5^{o} which correspond to the (111), (200) and (220) crystallographic planes of fcc using the Scherrer formula [32]:

$$D = \frac{K\lambda}{\beta \mathrm{Cos}\theta}, \quad (1)$$

where D corresponds to the crystal size, K is the shape-dependent Scherrer's constant (0.98), λ is the wavelength of radiation (0.15,406 nm) used for the XRD, β is the full peak width at half-maximum (FWHM) of the peak and θ is the Bragg's diffraction angle.

Catalytic application of Pt@Cu nanostructures

Preparation of model oil

Model oil containing 1 g/L sulfur dibenzothiophene (DBT) (98%) was prepared by dissolving 2.9 g of DBT in 500 mL *n*-heptane. The required concentration of sulfur solution was then prepared from stock solution by diluting with *n*-heptane.

Oxidation of model oil

The oxidation of model oil (DBT dissolved in *n*-heptane) into the corresponding sulfone or sulfoxide using H_2O_2 as oxidant was used as the probe reaction wherein the catalytic activity of the synthesized Pt@Cu nanostructures and acetic acid were compared.

In a typical reaction, specific amount of each catalyst [50 mg of Pt@Cu nanostructures or 15 mL of acetic acid (97%)] were separately added to 30 mL of H_2O_2 solution containing 30 mL (0.003 mmol) of the model oil (DBT dissolved in *n*-heptane) and the mixture was stirred at 60 °C for 2 h [33]. After the required time, the mixture was cooled rapidly to room temperature, transferred to a separating funnel and the upper phase (model oil) was withdrawn. The half portion of it was preserved for the analysis of sulfones and sulfoxides using FTIR, and the rest was extracted with distilled water twice and then with 20 mL 80% acetonitrile solution. The extracted sample was analyzed by Inductively Coupled Plasma Optical Emission Spectrometry (ICP-OES 5300DV) Perkin Elmer model, to determine the concentration of sulfur in the model oil. Then % removal of sulfur was calculated by the following equation:

$$\%\,\text{sulphur removal} = \frac{[\mathrm{DBT}]_i - [\mathrm{DBT}]_f}{[\mathrm{DBT}]_i} \times 100, \quad (2)$$

where $[\mathrm{DBT}]_i$ is the blank sample (without catalyst), and $[\mathrm{DBT}]_f$ is the catalytically oxidized DBT.

Results and discussion

UV–visible spectroscopy

Bioreduction of Pt and Cu ions to Pt@Cu nanostructures on exposure to *Alchornea laxiflora* leaf extract (ALLE) was monitored by visual observation of the color change and with UV–visible spectroscopy. There was gradual color change from bluish yellow solution of Pt(IV)–Cu(II) ions mixture to dark brown colloidal solution indicating the formation of Pt^0–Cu^0 as bioconversion proceeded at elevated temperature of 100 °C. The entire reaction was completed in 5 h. The final black color was ascribed to the excitation of surface plasmon vibrations in the Pt@Cu nanostructures, indicating the formation of Pt@Cu nanostructures. Figure 1 shows the color of *Alchornea laxiflora* leaf extract (a), the color of the mixture of chloroplatinic acid and copper sulfate containing solution before the reaction (b) and color of Pt@Cu nanostructures formed on completion of the reaction (c). In this study, *A. laxiflora* leaf extracts (ALLE) was used as both reducing and stabilizing agent for Pt@Cu formation. Generally, ALLE contains several polyphenolic and flavonoid compounds, such as quercetin, alkaloids, saponin and reducing sugars [34, 35], which can act as reducing and stabilizing agents.

Figure 2 shows the UV–visible spectra of ALLE, precursors H_2PtCl_6 and $CuSO_4{\cdot}5H_2O$ solutions, and the Pt@Cu nanostructures obtained by aqueous ALLE after reaction periods of 5 h at 100 °C. The UV spectrum of ALLE (Fig. 2a) shows bands at λ_{max} 203 nm (K-band) and

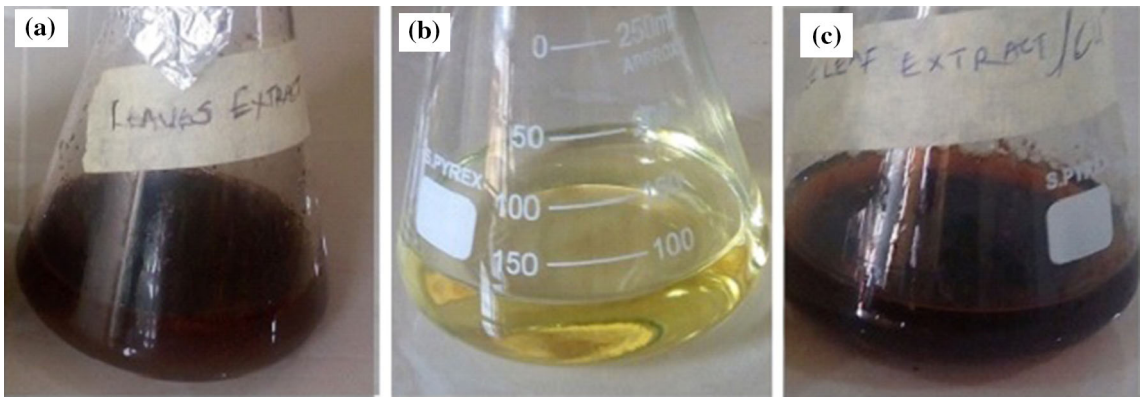

Fig. 1 Photographs showing the color of the tree leaf extract of *A. laxiflora* (**a**), solution Pt and Cu ions mixture (**b**) and colloidal Pt@Cu nanostructures (**c**)

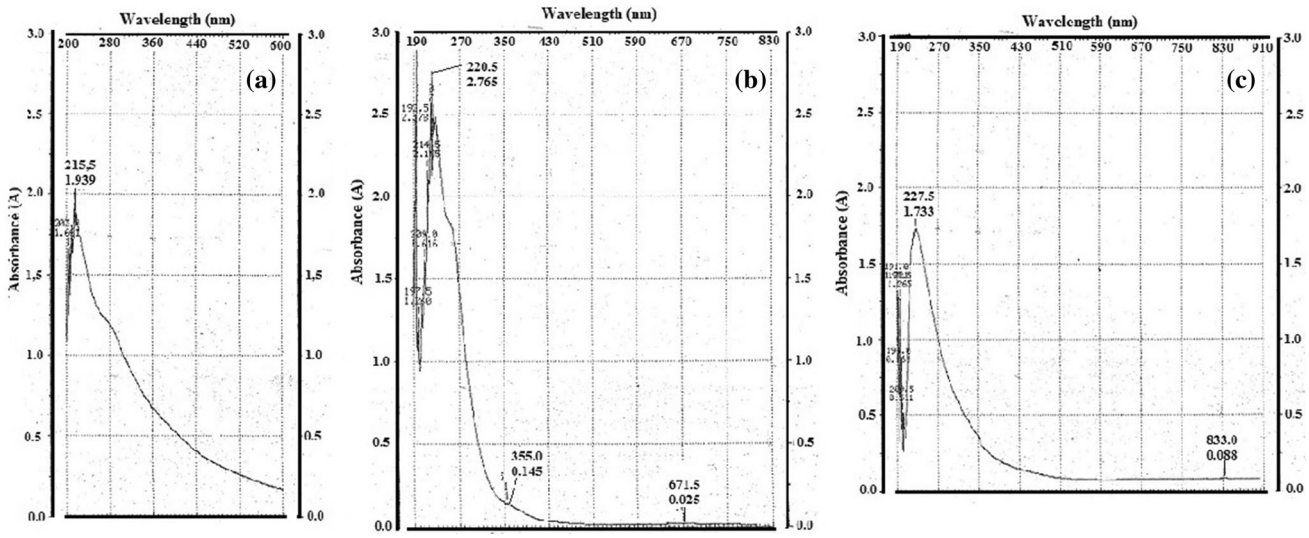

Fig. 2 UV–visible spectra of aqueous leaf extract of *Alchornea laxiflora* (**a**), platinum and copper ions mixture (**b**) and Pt@Cu nanostructures (**c**)

215 nm (band II). The band at 203 nm (K-band) can be due to $\pi \rightarrow \pi^*$ transition of the absorbance of ring related to the benzoyl system whereas the band at 215 nm (band II) can either be due to $n \rightarrow \pi^*$ transition or a combination of $\pi \rightarrow \pi^*$ and $n \rightarrow \pi^*$ transitions of heteroatoms linked in the double bond. Akinpelu et al. [34] reported the presence of phytoconstituents in the leaf extract of *Alchornea laxiflora* to include flavonoids, alkaloids, saponin and reducing sugars, while others reported the presence of quercetin, a class of flavonoid as major constituents of the crude methanolic leaf extract of *A. laxiflora* [35]. Therefore, the observed transitions are probably related to these bioactive compounds in ALLE which are involved in the reduction process and formation of Pt@Cu nanostructures via π-electron interactions [36, 37]. Hence, the aqueous extract of *Alchornea laxiflora* leaf acts as a reductant and stabilizer agent.

The platinum and copper ions mixture before reduction shows peaks at 220, 355 and 671 nm in its UV–vis spectrum (Fig. 2b) due to the ligand-to-metal charge transfer transition of the mixed $[PtCl_6]^{-2}$ and Cu^{2+} ions. The peaks at 220, 355 and 671 nm disappeared after the reduction, indicating that $[PtCl_6]^{-2}$ and Cu^{2+} ions mixture have been reduced completely. The surface plasmon resonance (SPR) of PtNPs is found in the ultraviolet range at around 215 nm, unlike other noble metal nanoparticles which display SPR in the visible range [38] while the surface plasmon resonance (SPR) peak that is a signature of the formation of Cu nanoparticles appears in visible region [39, 40]. The Pt@Cu nanostructures had absorption at 227 and 833 nm in its UV–vis spectrum (Fig. 2c), corresponding to the SPR peaks of pure Pt and pure Cu, respectively.

HRTEM and EDX

High resolution transmission electron microscopy (HRTEM) was used to characterize the lattice arrangement and crystallinity of the Pt@Cu nanostructures. Figure 3 shows the HRTEM image of the as-synthesized Pt@Cu nanostructures. The Pt@Cu nanostructures exhibit highly uniform morphology and the sizes range between 1.87 and 2.38 nm with average particles size of 2.12 ± 0.21 nm. The particles were well stabilized in the matrix of biomaterial with no sign of agglomeration.

The presence of metallic platinum and copper in EDX pattern (Fig. 4) reflects bimetallic nature and it reveals that the atomic ratio between Pt and Cu is about 2:3 as calculated from the EDX quantitative data (Table 1). The EDX pattern also shows presence of carbon (63.46%), oxygen (3.57%), and nitrogen (4.72%), as other elements, which may originate from bioactive molecules in ALLE that surround Pt@Cu nanostructures surface, and also help in protecting the Pt@Cu nanostructures from agglomeration.

XRD analysis

The crystalline nature of the as-synthesized Pt@Cu nanostructures was further confirmed using XRD analysis. Figure 5 shows the XRD spectrum corresponding to the powdered Pt@Cu nanostructures synthesized by *Alchornea laxiflora* leaf extract at 100 °C. The x-ray diffraction consists of peaks at 39.8°, 47.6° and 67.5°, corresponding to reported single fcc Pt phase [38, 41], while peaks at 43.7°, 50.7° and 74.5° correspond to reported single fcc Cu phase [40, 41]. The reflection observed at 45.2°, 57° and 68.5° are assigned to the Miller diffraction plane at (111), (200) and (220), respectively, for the Pt@Cu nanostructures system, which confirmed that they are crystallized in face-centered cubic phase (f*cc*) structure [42–44]. The average crystal size was calculated using Scherrer's equation and estimated as 2.46 nm, which closely agrees with the average particle size of 2.12 nm obtained from HRTEM. The peaks observed at 2 θ values of 22°, 31° and 32° can be ascribed to the elemental composition in ALLE that are acting as capping and stabilizing agents for bimetallic Pt@Cu nanostructures, thus preventing agglomeration.

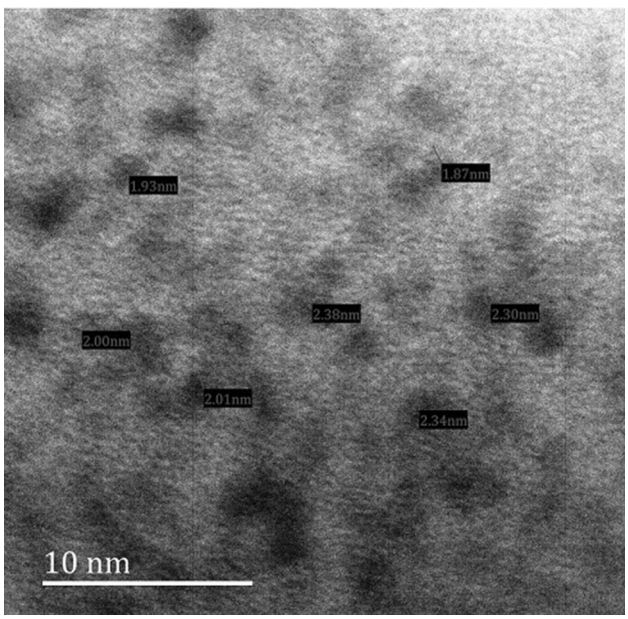

Fig. 3 HRTEM image of Pt@Cu bimetallic nanostructures

Fourier transform infrared spectroscopy(FTIR)

The FTIR analysis of aqueous leaf extract of *Alchornea laxiflora* was carried out to identify the possible biomolecules responsible for the reduction of Pt^{4+}–Cu^{2+} to $Pt^0@Cu^0$ nanostructures as well as the capping and stabilizing agents for Pt@Cu nanostructures. The FTIR spectrum of the aqueous leaf extract (Fig. 6a) shows a broad peak at 3427 cm^{-1} which can be assigned to the stretching vibration of O–H of phenolic compound, while the weak peak at 2368 cm^{-1} indicates the presence of C ≡ N or C ≡ C stretching vibration. The sharp peak at 1635 cm^{-1} is attributed to conjugated carbonyl (> =C=O) stretching vibration of carboxylic acid/lactones or C=C stretching vibration of aromatic ring. The characteristic peaks at 1438, 1118 and 613 cm^{-1} can be assigned to in-plane OH bending of carboxylic acids, C–O stretch of phenol and C–H bend of aromatic compounds or alkynes, respectively. These peaks suggested the presence of flavonoids and other polyphenolic compounds in the aqueous leaf extract of *A. laxiflora*, which could be responsible for the reduction of Pt^{4+}–Cu^{2+} ion mixture to their corresponding Pt@Cu bimetallic nanostructures.

The FTIR spectrum of as-synthesized Pt@Cu nanostructures is shown in Fig. 6b. The formation of Pt@Cu nanostructures shows distinctive differences in the shape and positions of peaks, indicating the existence of interaction between Pt^{4+} and Cu^{2+} ion mixture and the responsible functional group of phytoconstituents for the synthesis of Pt@Cu nanostructures. There are appearances of new peaks at 3950 and 3749 cm^{-1} which represent the N–H stretching vibration of amines. The broad peak observed for the aqueous leaf extract at 3427 cm^{-1} which is due to OH stretching vibration disappeared completely in the spectrum of as-synthesized Pt@Cu which could be due to the involvement of this functional group in bioreduction process. Other new peaks at 2380, 2341 and 1845 cm^{-1} can be ascribed to C ≡ N or C ≡ C stretching vibration and >C=O stretching vibration of carbonyl compounds,

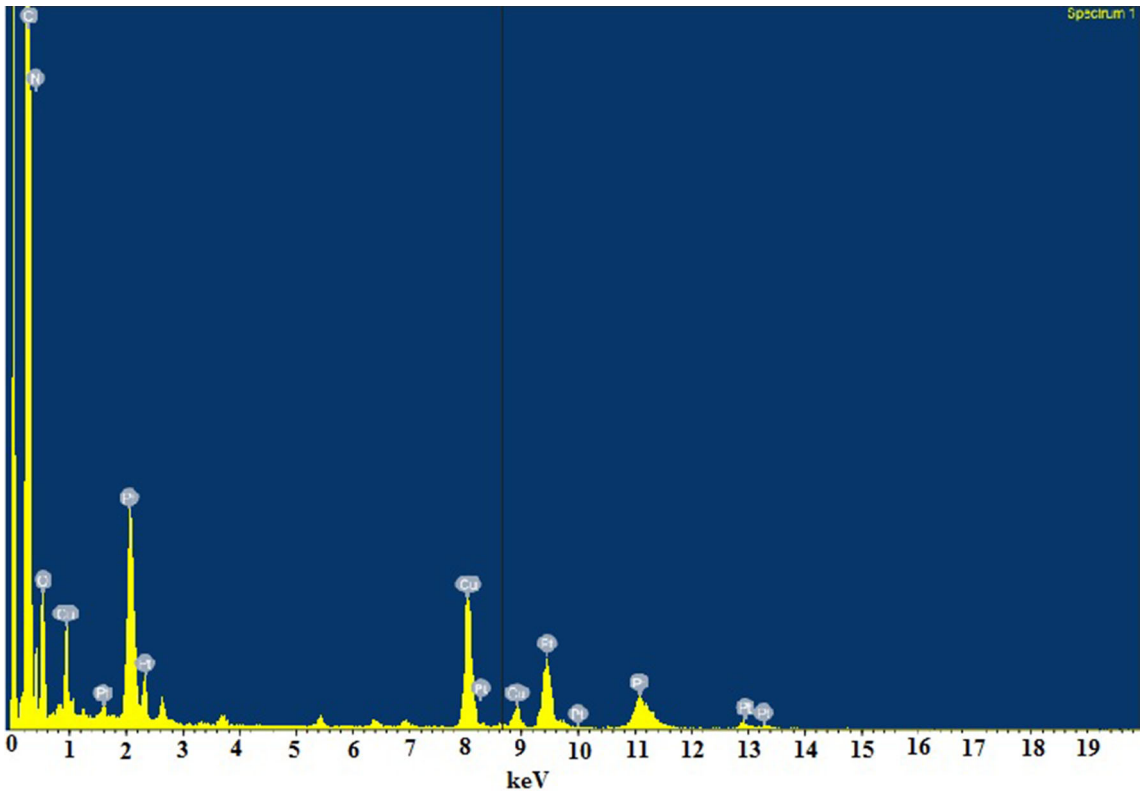

Fig. 4 Energy dispersive X-ray patterns of bimetallic Pt@Cu nanostructures

Table 1 EDX result for the as-synthesized Pt@Cu nanostructures using *A. laxiflora* leaf extract

Element	Weight (%)	Atomic (%)
C K	63.46	86.21
N K	4.72	5.49
O K	3.57	3.65
S K	0.93	0.48
Cl K	0.70	0.32
Ca K	0.25	0.10
Cr K	0.32	0.10
Fe K	0.26	0.08
Co K	0.20	0.06
Cu K	7.71	1.98
Zn K	0.26	0.06
Pt L	16.35	1.37
Au L	1.25	0.10

respectively. The sharp peak observed for the aqueous leaf extract at 1635 cm^{-1} also slightly shifted to 1637 cm^{-1} in the spectrum of bimetallic Pt@Cu nanostructures, and could be ascribed to >C=C< stretching vibration of aromatic ring. Peaks at 1463–1319 cm^{-1} could be assigned to CH_3 antisymmetric deformation in aliphatic compounds or in-plane OH bending vibration of carboxylic acids. The peak at 1118 cm^{-1} could be ascribed to C–O stretching vibration of ester. The band at 574 cm^{-1} corresponds to Cu–O stretching vibration.

The bioreduction mechanism of the aqueous plant leaf extract is believed to be due to the presence of the bioactive molecules such as quercetin, proteins, polyphenolic compounds, terpenoids and reducing sugars in the aqueous leaf extract [45–47]. In the present investigation, it was evidenced from FTIR analysis that the reduction of platinum and copper ions mixture was predominantly performed by the O–H functional group of quercetin, which has been identified as one of the bioactive chemical constituents isolated from the crude methanolic leaf extract of *A. laxiflora* [34, 35]. The possible reaction mechanism of quercetin with mixture of platinum and copper ions, accepting electrons and get converted into pure platinum (Pt^0) and pure copper (Cu^0) is hereby proposed (Scheme 2).

It could be observed from the mechanism that the π-electrons of the aromatic ring can transfer electrons to the partially filled *d*-orbital of Pt^{4+} and Cu^{2+} ions, which are then converted into free platinum and copper (Scheme 2).

During the bioreduction, all the O–H functional groups in quercetin, the bioactive molecule in the aqueous leaf extract of *A. laxiflora,* were converted to quinones and this

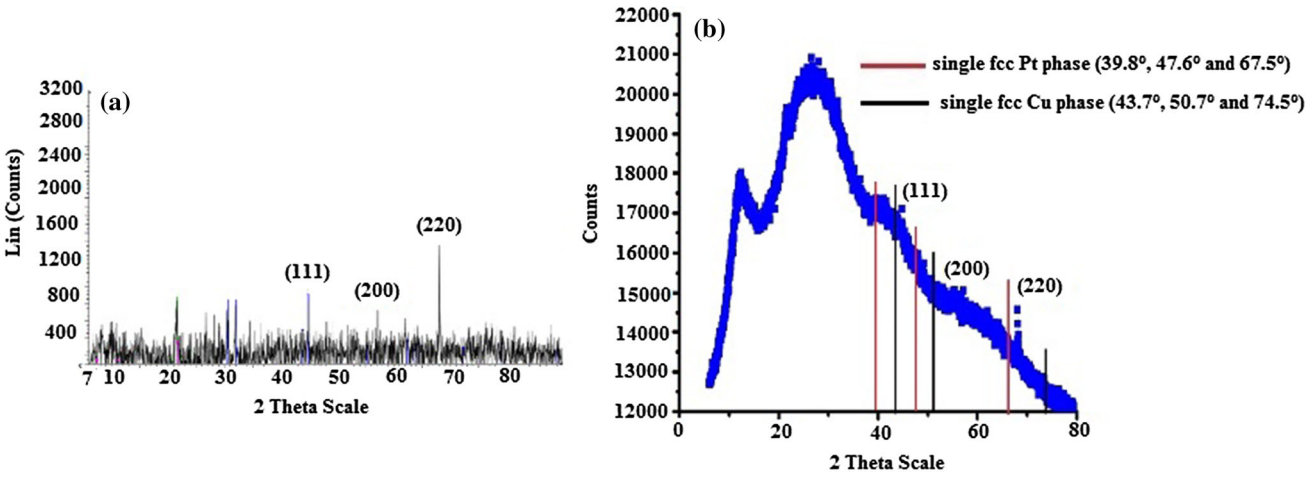

Fig. 5 X-Ray diffraction gragh (**a**) and OriginPro 8 Software plot (**b**) of as-synthesized Pt@Cu nanostructures using ALLE at 100 °C

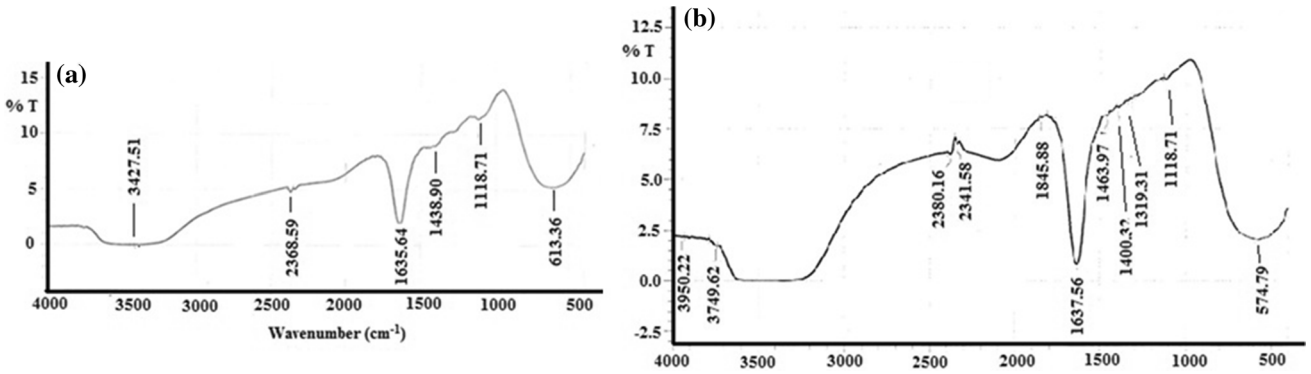

Fig. 6 FTIR spectra of aqueous leaf extract of *Alchornea laxiflora* (**a**), and Pt@Cu bimetallic nanostructures (**b**)

led to complete disappearance of the OH band in the FTIR spectrum of the Pt@Cu nanostructures and appearance of new at 1845 cm^{-1} in the FTIR spectrum of Pt@Cu bimetallic, which was assigned to >C=O stretch of cyclic ketones (Fig. 6b). The FTIR spectrum (Fig. 6b) also confirmed the presence of N–H, C ≡ N, >C=O, and C ≡ C groups, corresponding to the presence of metabolites, protein, ketones and carboxylic acid that surround the bimetallic Pt@Cu nanostructures as capping and stabilizing agents. Our observation is in agreement with those of other researchers [48–51] who have also reported that the carbonyl groups from amino acid residues or protein strongly bind to metal nanoparticles as capping agent and stabilize the nanoparticles by preventing their agglomeration.

Catalytic activity of Pt@Cu nanostructures in the oxidative desulfurization of model oil

Here, we evaluated the catalytic activity of the bimetallic Pt@Cu nanostructures for the oxidative desulfurization of model oil by comparing its catalytic activity with that of the conventional acetic acid catalyst. The oxidation reaction of model oil (DBT dissolved in *n*-heptane) was carried out separately in the presence of bimetallic Pt@Cu nanostructures and acetic acid as catalysts at elevated temperature of 60 °C followed by FTIR analysis and total sulfur determination of the desulfurized product. The FTIR spectrum of the model oil (Fig. 7a) shows sharp bands at 2956, 2924 and 2866 cm^{-1} indicating methyl and methylene C–H bonds followed by strong absorption bands at 1460 and 1377 cm^{-1} representing methylene C–C stretching vibration. The weak bands at 732, 634 and 570 cm^{-1} are due C–S stretching vibration of dibenzothiophene.

The FTIR spectra of the oxidized products (Fig. 7 b, c) show weak bands at 1392 and 1367 cm^{-1} for the acetic acid and bimetallic Pt@Cu nanostructures catalyzed reactions, respectively, which are typical absorption for the asymmetric stretching vibration of sulfone, and may correspond to the bond associated with DBT sulfone, followed by strong absorption bands at 3317 and 3296 cm^{-1}, respectively, indicating the presence of OH which may be from H_2O_2 decomposition. The Pt@Cu–catalyzed reaction gave additional weak band at 1147 cm^{-1}, which can be

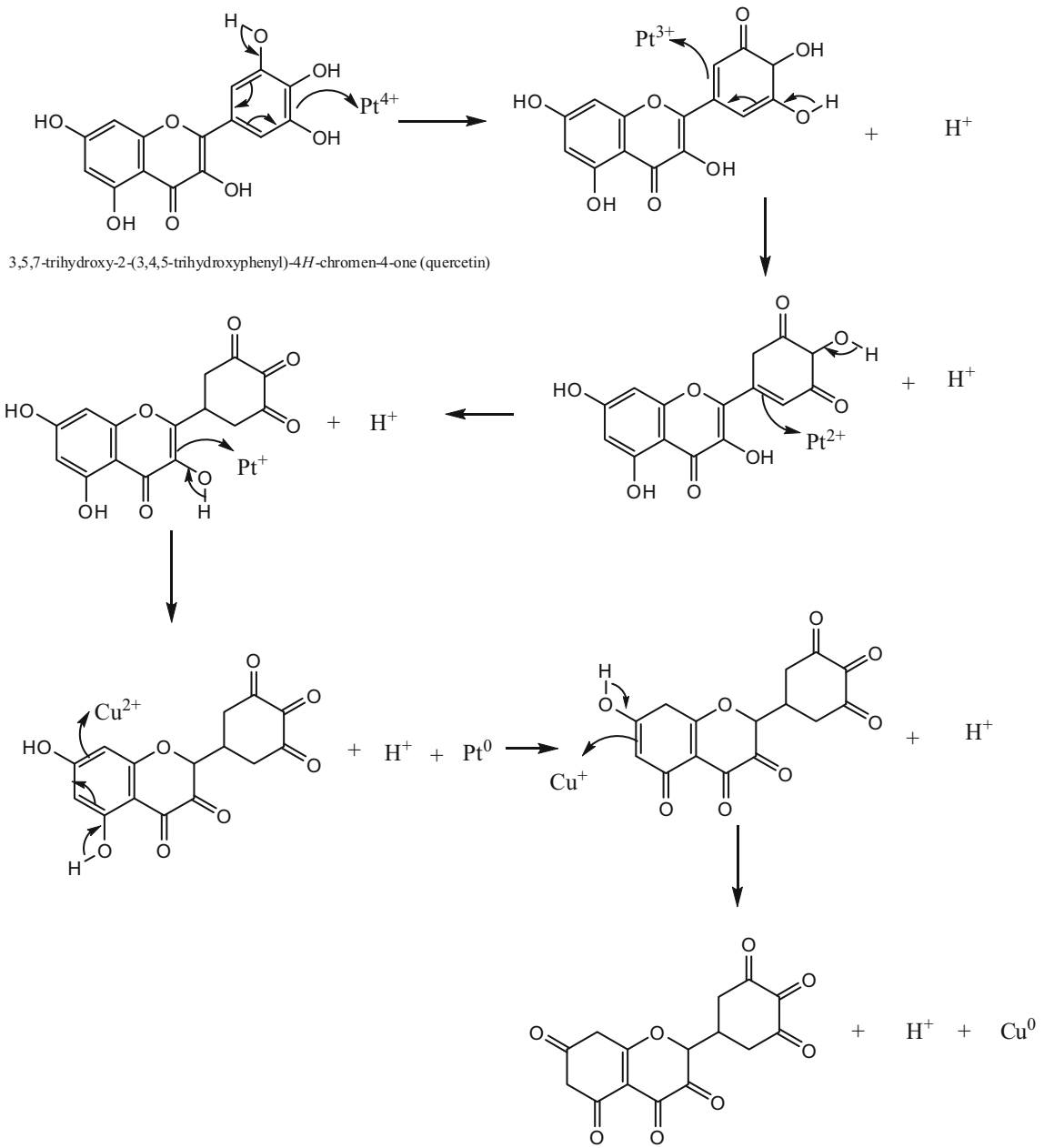

Scheme 2 Proposed mechanism for the bioreduction of Pt^{4+} and Cu^{2+} ions mixture to Pt and Cu by a typical polyphenolic compound in *Alchornea laxiflora* leaf extract (ALLE)

ascribed to symmetrical stretching vibration of DBT sulfone. There are sharp bands positioned at 1637 cm^{-1} for both acetic acid and Pt@Cu nanostructures catalyzed reactions, which can be ascribed to >C=C< stretching vibration of aromatics, followed by weak bands at 1843 and 1923 cm^{-1}, respectively, which are due to C–H bending vibration of aromatic compound. Dibenzothiophene was exclusively converted to DBT sulfone with no formation of DBT sulfoxide as evidenced from the absence of typical sulfoxide bands in the range 1039–1050 cm^{-1} in the FTIR spectra of the oxidized DBT products (Fig. 7b, c).

A quantitative analysis of the chemical composition of DBT on oxidation, which reflects the oxidative desulfurization efficiency of two catalysts used in this study, was calculated using the formula [52]:

$$I_{SO_2}(\%) = \frac{A_{SO_2}}{\sum A_T} \times 100, \quad (3)$$

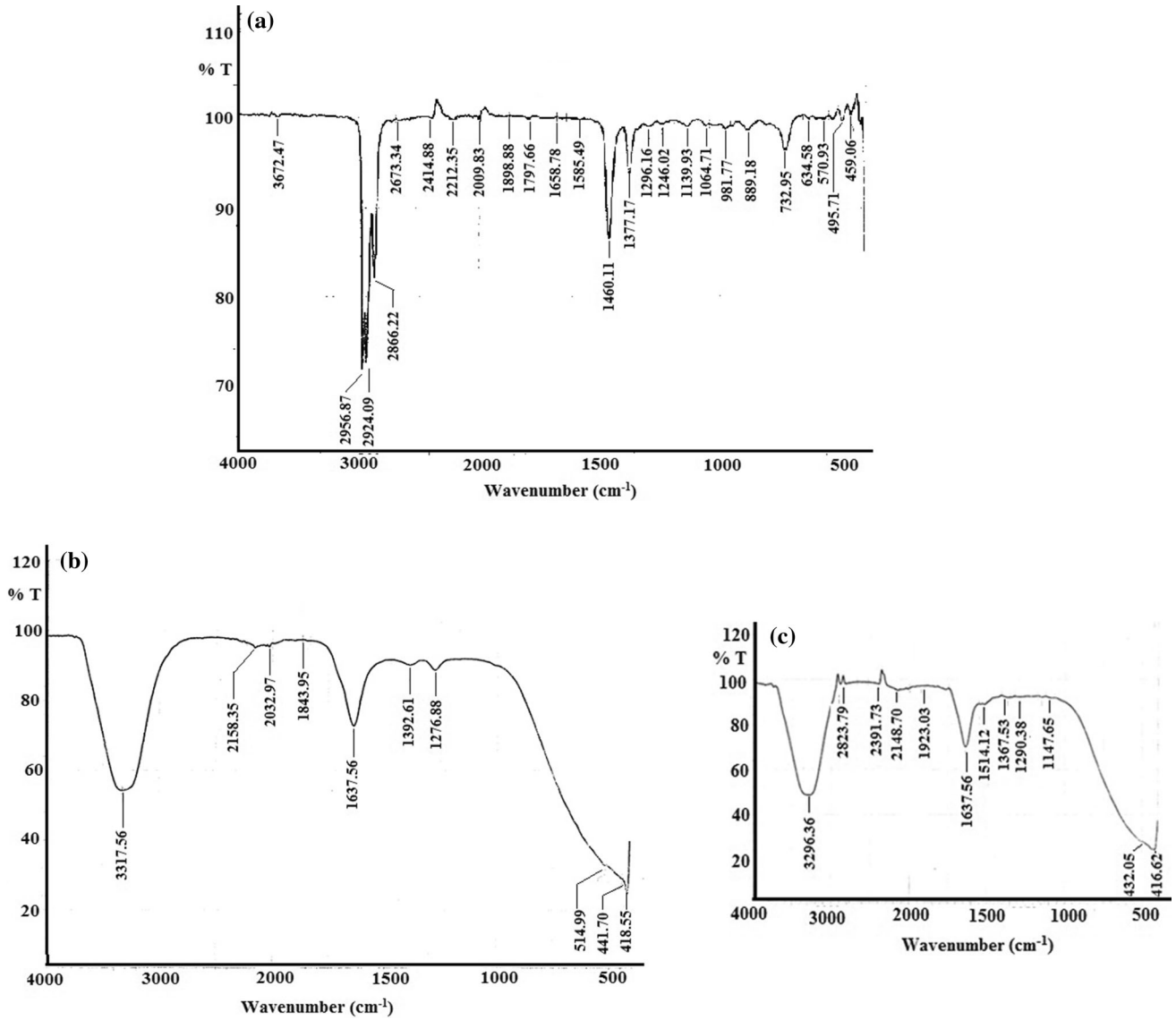

Fig. 7 FTIR spectra of model oil (**a**), acetic acid-catalyzed ODS (**b**), and Pt@Cu bimetallic nanostructures-catalyzed ODS (**c**)

where I_{SO_2} is the sulfone index; $\sum A_{SO_2}$ is sum of the area of spectra bands for asymmetrical stretch (1420–1300 cm^{-1}), symmetric stretch (1200–1100 cm^{-1}) and bending vibration (600–540 cm^{-1}) of the sulfone; while $\sum A_T$ is the total sum of the area of spectra bands between 2000 and 600 cm^{-1}. The functional groups identifiable in this wavelength range for DBT sulfone as extracted from their FTIR spectra (Fig. 7b, c) are given in Table 2.

In the present study, however, DBT sulfone shows asymmetric stretch and symmetrical stretch (only for Pt@Cu-based catalyst) in their FTIR spectra, and this was used for calculating the sulfone index. The calculated sulfone index which was used to compare the sulfur content of DBT sulfone gave values of 1.06 and 3.5% for Pt@Cu nanostructures and acetic acid, respectively, thus indicating that bimetallic Pt@Cu nanostructures has higher desulfurization efficiency than acetic acid. This observation was further confirmed from the total sulfur contents of

Table 2 Functional groups extracted from FTIR spectra of DBT sulfone

Functional group	Typical absorption (cm^{-1})
Sulfone	1420–1300 (asymm.)
Aromatic C=C stretch	1200–1100 (symm.)
C–S stretch	600–540 (bending)
C–H bending (oop)	1650–1600
C–H bending of aromatic (overtones)	700–600
	900–700 (weak)
	2000–1660 (weak)

Table 3 Sulfur contents after oxidation of model oil with acetic acid and bimetallic Pt@Cu nanostructures catalysts

Catalysts	Residual Sulfur in the oxidized model oil (mg/L)	Sulfur removal (%)
Blank (no catalyst)	19.490 ± 0.409	–
Acetic acid	14.064 ± 0.257	27.8
Pt@Cu nanostructures	2.009 ± 0.346	89.69

DBT sulfone (Table 3), where bimetallic Pt@Cu nanostructures have higher percent sulfur removal (89.69%) than acetic acid (27.8%).

The synergistic electronic effect operating at the interface of the two metals in bimetallic Pt@Cu nanostructures may account for the observed enhanced performance of their catalytic activity [53, 54]. It is, therefore, concluded that bimetallic Pt@Cu nanostructures have greater catalytic performance than acetic acid. Thus, bimetallic Pt@Cu nanostructures can be used as inexpensive alternative catalytic materials in the petroleum industry for oxidative desulfurization of model oil.

Conclusion

We have demonstrated a simple, an eco-friendly method for the synthesis of bimetallic Pt@Cu nanostructures using *Alchornea laxiflora* leaf extract (ALLE). HRTEM analysis reveals the average particle size of the synthesized bimetallic Pt@Cu nanostructures to be 2.12 ± 0.21 nm with uniform morphology. The as-synthesized Pt@Cu nanostructures were utilized as catalyst for the oxidation of dibenzothiophene using H_2O_2 as oxidant and their catalytic potential were compared with the conventional acetic acid catalyst. It was found that the bimetallic nanostructures have threefold higher catalytic potential compared to the conventional acetic acid catalyst. These bimetallic nanostructures can, therefore, be utilized as inexpensive alternative catalytic materials in the petroleum industry for ODS process.

Acknowledgements All thanked Technologists of Research Centre of the University of KwaZulu-natal, South Africa for their Technical assistance. This research is self-sponsored and did not receive any grant from funding agencies either in the public, commercial or non-profit sectors.

Compliance with ethical standards

Conflict of interest There are no competing interests.

References

1. Salunke, G.R., Ghosh, S., Santosh Kumar, R.J., Khade, S., Vashisth, P., Kale, T., Chopade, S., Pruthi, V., Kundu, G., Bellare, J.R., Chopade, B.A.: Rapid efficient synthesis and characterization of silver, gold, and bimetallic nanoparticles from the medicinal plant *Plumbago zeylanica* and their application in biofilm control. Int. J. Nanomed. **9**, 2635–2653 (2014)
2. Gaidhani, S., Singh, R., Singh, D., Patel, U., Shevade, K., Yeshvekar, R.: Chopade, B.A: biofilm disruption activity of silver nanoparticles synthesized by *Acinetobacter calcoaceticus* PUCM 1005. Mater. Lett. **108**, 324–327 (2013)
3. Gaidhani, S.V., Yeshvekar, R.K., Shedbalkar, U.U., Bellare, J.H., Chopade, B.A.: Bio-reduction of hexachloroplatinic acid to platinum nanoparticles employing *Acinetobacter calcoaceticus*. Process Biochem. **49**(12), 2313–2319 (2014)
4. Shedbalkar, U., Singh, R., Wadhwani, S., Gaidhani, S., Chopade, B.A.: Microbial synthesis of gold nanoparticles: current status and future prospects. Adv. Colloid Interface Sci. **209**, 40–48 (2014)
5. Singh, R., Wagh, P., Wadhwani, S., Gaidhani, S., Kumbhar, A., Bellare, J., Chopade, B.A.: Synthesis, optimization, and characterization of silver nanoparticles from *Acinetobacter calcoaceticus* and their enhanced antibacterial activity when combined with antibiotics. Int. J. Nanomed. **8**, 4277–4290 (2013)
6. Singh, R., Nawale, L.U., Arkile, M., Shedbalkar, U.U., Wadhwani, S.A., Sarkar, D., Chopade, B.A.: Chemical and biological metal nanoparticles as antimycobacterial agents: a comparative study. Int. J. Antimicrob. Agents **46**(2), 183–188 (2015)
7. Wadhwani, S.A., Shedbalkar, U.U., Singh, R., Karve, M.S., Chopade, B.A.: Novel polyhedral gold nanoparticles: green synthesis, optimization and characterization by environmental isolate of *Acinetobacter* sp. SW30. World J Microbiol. Biotechnol. **30**(10), 2723–2731 (2014)
8. Sant, D.G., Gujarathi, T.R., Harne, S.R., Ghosh, S., Kitture, R., Kale, S., Chopade, B.A., Pardesi K.R.: *Adiantum philippense L.* frond assisted rapid green synthesis of gold and silver nanoparticles. J. Nanoparticles. **2013**, 9 (2013)
9. Thakkar, K.N., Mhatre, S.S., Parikh, R.Y.: Biological synthesis of metallic anoparticles. Nanomed. Nanotech. Bio. Med. **6**, 257–262 (2010)
10. Lim, S., Hudson, S.M.: Application of a fiber-reactive chitosan derivative to cotton fabric as an antimicrobial textile finish. Carbohydr. Polym. **56**, 227–234 (2004)
11. Pattanayak, M., Nayak, P.L.: Green synthesis and characterization of zero valent iron nanoparticles from the leaf extract of *Azadirachta indica* (Neem). World J. Nanosci. Techol. **2**(1), 6–9 (2013)
12. Kim, N.R., Shin, K., Jung, I., Shim, M., Lee, M.: Ag-Cu bimetallic nanoparticles with enhanced resistance to oxidation: a combined experimental and theoretical study. J. Phys. Chem. C **118**, 26324–26331 (2014)
13. Sopoušek, J., Pinkas, J., Brož, P., Buršík, J., Vykoukal, V., Škoda, D., Stýskalík, A., Zobač, O., Vřešťál, J., Hrdlička, A., Šimbera, J.: Ag-Cu colloid synthesis: Bimetallic nanoparticle characterisation and thermal treatment. J. Nanomater. **2014** (2014). doi:10.1155/2014/638964

14. Wang, D., Li, Y.: Bimetallic nanocrystals: bimetallic nanocrystals: liquid-phase synthesis and catalytic applications. Adv. Mater. **23**, 1036 (2011)
15. Yang, H.: Platinum-based electrocatalysts with core–shell nanostructures. Angew. Chem. Inter. Ed. **50**, 2674–2676 (2011)
16. Zhang, H., Jin, M., Xia, Y.: Enhancing the catalytic and electrocatalytic properties of Pt-based catalysts by forming bimetallic nanocrystals with Pd. Chem. Soc. Rev. **41**, 8035–8049 (2012)
17. Singh, A.K., Xu, Q.: Synergistic catalysis over bimetallic alloy nanoparticles. Chem. Cat. Chem **5**, 652–676 (2013)
18. Zhou, K., Li, Y.: Catalysis based on nanocrystals with well-defined facets. Angew. Chem. Int. Ed. **51**, 602–613 (2012)
19. Porter, N.S., Wu, H., Quan, Z., Fang, J.: Shape-control and electrocatalytic activity-enhancement of Pt-based bimetallic nanocrystals. Acc. Chem. Res. **46**, 1867–1877 (2013)
20. Kang, S., Gao, G., Xie, X., Shibayama, T., Lei, Y., Wang, Y., Cai, L.: Synthesis of surfactant-free Cu–Pt dendritic heterostructures with highly electrocatalytic performance for methanol oxidation reaction. Mater. Res. Lett. **4**(4), 212–218 (2016)
21. Singh, H.P., Gupta, N., Sharma, S.K., Sharma, R.K.: Synthesis of bimetallic Pt–Cu nanoparticles and their application in the reduction of rhodamine B. Colloids Surf. A Physicochem. Eng. Asp. **416**, 43–50 (2013)
22. Taylor, E., Chen, S., Tao, J., Wu, L., Zhu, Y., Chen, J.: Synthesis of Pt–Cu nanodendrites through controlled reduction kinetics for enhanced methanol electro- oxidation. Chem. Sus Chem. **6**(10), 1863–1867 (2013)
23. Liu, B., Zhu, Y., Liu, S., Mao, J.: Adsorption equilibrium of thiophenic sulfur compounds on the Cu- BTC metal-organic framework. J. Chem. Eng. Data **57**(4), 1326–1330 (2012)
24. Qi, Y., Bian, T., Choi, S.-I., Jiang, Y., Jin, C., Fu, M., Zhang, H., Yang, D.: Kinetically controlled synthesis of Pt-Cu alloy concave nanocubes with high-index facets for methanol electro-oxidation. Chem. Commun. **50**, 560–562 (2014)
25. Wang, Y., Li, G., Wang, X., Jin, C.: Oxidative Desulphurization of 4,6 dimethyldibenzothiophene with hydrogen peroxide over Ti-HMS. Energy Fuels **21**, 1415–1419 (2007)
26. Zhu, W., Li, H., Jiang, X., Yan, Y., Lu, J., Xia, J.: Oxidative desulfurization of fuels catalyzed by peroxotungsten and peroxomolybdenum complexes in ionic liquids. Energy Fuels **21**, 2514–2516 (2007)
27. Di Giuseppe, A., Crucianelli, M., De Angelis, F., Crestini, C., Saladino, R.: Efficient oxidation of thiophene derivatives with homogeneous and heterogeneous MTO/H_2O_2 systems: a novel approach for, oxidative desulfurization (ODS) of diesel fuel. Appl. Catal. B: Environ. **89**, 239–245 (2009)
28. Palaić, N., Sertić-Bionda, K., Margeta, D., Podolski, Š.: Oxidative desulphurization of diesel fuels. Chem. Biochem. Eng. Q **29**(3), 323–327 (2015)
29. Wang, D., Qian, E.W., Amano, H., Okata, K., Ishihara, A., Kabe, T.: Oxidative desulphurization of fuel oil: part 1. Oxidation of dibenzothiophenes using tert-butyl hydroperoxide. Appl. Catal. A Gen **263**, 91–99 (2003)
30. Wang, J., Zhao, R., Han, B., Tang, N., Li, K.: Extractive and oxidative desulphurization of model oil in polyethylene glycol. RSC Adv. **6**(41), 35071–35075 (2016)
31. Jiang, Z., Lu, H., Zhang, Y., Li, C.: Oxidative desulphurization of fuel oils. Chin. J. Catal. **32**, 707–715 (2011)
32. Monshi, A., Foroughi, M.R., Monshi, M.R.: Modified scherrer equation to estimate more accurately nano-crystallite size using XRD. World J. Nano Sci. Eng. **2**, 154–160 (2012)
33. Mohammad, F.A., Abdullah, A., Bassam, E.A.: Deep desulphurization of gasoline and diesel fuels using non-hydrogen consuming techniques. Fuel **86**, 1354–1363 (2006)
34. Akinpelu, O.A., Abioye, E.O., Aiyegoro, O.A., Akinpelu, O.E., Okoh, A.I.: Evaluation of antibacterial and antifungal properties of *Alchornea laxiflora* (Benth.) Pax. & Hoffman. Evid. Based Complement. Altern. Med. (2015). doi:10.1155/2015/684839
35. Ogundipe, O.O., Moody, J.O., Houghton, P.J., Odelola, H.A.: Bioactive chemical constituents from *Alchornea laxiflora* (benth) pax and Hoffman. J. Ethnopharm. **74**(3), 275–280 (2001)
36. Nasrollahzadeh, M., Enayati, M., Khalaj, M.: Synthesis of N-arylureas in water and their *N*-arylation with halides using copper nanoparticles loaded on natural Natrolite zeolite under ligand-free conditions. RSC Adv. **4**, 26264–26270 (2014)
37. Nasrollahzadeh, M., Sajadi, S.M., Rostami-Vartooni, A., Khalaj, M.: Green synthesis of palladium nanoparticles using *Hippophae rhamnoides* Linn leaf extract and their catalytic activity for the Suzuki-Miyaura coupling in water. J. Mol. Catal. A Chem. **396**, 31–39 (2015)
38. Stepanov, A.L., Golubev, A.N., Nikitin, S.I., Osin, Y.N.: A Review on the fabrication and properties of platinum nanoparticles. Rev. Adv. Mater. Sci. **38**, 160–175 (2014)
39. Chan, G.H., Zhao, J., Hicks, E.M., Schatz, G.C., Van Duyne, R.P.: Plasmonic Properties of copper nanoparticles fabricated by nanosphere lithography. Nano Lett. **7**(7), 1947–1952 (2007)
40. Liu, P., Wang, H., Li, X., Rui, M., Zeng, H.: Localized surface plasmon resonance of Cu nanoparticles by laser ablation in liquid media. RSC Adv. (2015). doi:10.1039/C5RA14933A
41. Cao, Y., Yang, Y., Shan, Y., Huang, Z.: One-pot and facile fabrication of hierarchical branched Pt−Cu nanoparticles as excellent electrocatalysts for direct methanol fuel cells. ACS Appl. Mater. Interfaces (2016). doi:10.1021/acsami.5b11364
42. Chen, D.H., Chen, C.J.: Formation and characterization of Au–Ag bimetallic nanoparticles in water-in-oil microemulsions. J. Mater. Chem. **12**, 1557–1562 (2002)
43. Shah, A., Rahman, L.U., Qureshi, R., Rehman, Z.U.: Synthesis, characterization and applications of bimetallic (Au–Ag, Au–Pt, Au–Ru) alloy nanoparticles. Rev. Adv. Mater. Sci. **30**, 133–149 (2012)
44. Tamuly, C., Hazarika, M., Borah, SCh., Boruah, M.P., Das, M.R.: *In situ* biosynthesis of Ag, Au and bimetallic nanoparticles using Piper pedicellatum C.DC: green chemistry approach. Colloid Surf. B **102**, 627–634 (2013)
45. Castro, L., Blazquez, M.L., Munoz, J.A., Gonzalez, F., Garcıa-Balboa, C., Ballester, A.: Biosynthesis of gold nanowires using sugar beet pulp. Process Biochem. **46**, 1076–1082 (2011)
46. Marshall, A.T., Haverkamp, R.G., Davies, C.E., Parsons, J.G., Gardea-Torresdey, J.L., van Agterveld, D.: Accumulation of gold nanoparticles in *Brassic juncea*. Int. J. Phytoremed. **9**, 197–206 (2007)
47. Shah, M., Fawcett, D., Sharma, S., Tripathy, S.K., Poinern, G.E.J.: Green synthesis of metallic nanoparticles via biological entities. Materials **8**, 7278–7308 (2015)
48. Balaji, D.S., Basavaraja, S., Deshpande, R., Mahesh, D.B., Prabhakar, B.K., Venkataraman, A.: Extracellular biosynthesis of functionalized silver nanoparticles by strains of *Cladosporium cladosporioides* fungus. Colloids Surf. B **68**, 88–92 (2009)
49. Philip, D.: Biosynthesis of Au, Ag and Au–Ag nanoparticles using edible mushroom extract. Spectrochim. Acta A Mol. Biomol. Spectrosc. **73**, 374–381 (2009)
50. Mallikarjuna, K., Narasimha, G., Dillip, G., Praveen, B., Shreedhar, B., Sreelakshmi, C., Reddy, B., Deva, P.: Green synthesis of silver nanoparticles using Ocimum leaf extract and their characterization. J. Nanomater. Biostruct. **6**, 181–186 (2011)
51. Kasthuri, J., Veerapandian, S., Rajendiran, N.: Biological synthesis of silver and gold nanoparticles using apiin as reducing agent. Colloids Surf. B **68**, 55–60 (2009)
52. Lamontagne, J., Dumas, P., Mouillet, V., Kister, J.: Comparison by Fourier transform infrared (FTIR) spectroscopy of different

ageing techniques: application to road bitumen. Fuel **80**(4), 483–488 (2001)
53. Lee, Y., Garcia, M.A., Huls, N.A.F., Sun, S.: Synthetic tuning of the catalytic properties of Au–Fe_3O_4 nanoparticles. Angew. Chem. Int. Ed. **49**, 1271–1274 (2010)
54. Shao, M., Wang, H., Zhang, M., Ma, D.D.D., Lee, S.T.: The mutual promotional effect of Au–Pd bimetallic nanoparticles on the silicon nanowires: a study of preparation and catalytic activity. Appl. Phys. Lett. **93**, 243110 (2008)